

Two-electron temperature model of a laser-driven implosion

J. R. Sanmartín, R. Ramis, J. L. Montañés, and J. Sanz

Escuela Técnica Superior de Ingenieros Aeronáuticos, Universidad Politécnica de Madrid, Madrid-3, Spain

The plasma ejected by a pellet irradiated with moderately intense laser light ($I_{cr}\lambda^2 \sim 10^{15} \text{ W cm}^{-2} \mu\text{m}^2$, I_{cr} and λ being intensity and wavelength) is analyzed. Both hot electrons caused by resonant absorption, and cold or thermal electrons are considered; no appeal is made to heat-flux saturation. The cold (hot) population controls the overdense (underdense) plasma flow. Ingoing hot electrons at the critical surface are found to thermalize before reaching the ablation surface. Results obtained are compared with a model that assumes *one electron temperature, and a saturated flux*; agreement requires using a range of saturation factors: $0.1 \lesssim f \lesssim 0.3$. The validity of the model is discussed.

I. INTRODUCTION

A quasisteady fluid model was used in the past to analyze the coronal plasma ejected by a laser-irradiated pellet.¹⁻⁴ The quasisteady assumption, discussed by Max *et al.*,³ holds if a fluid particle crosses the corona in a time, of order $r_{cr}/v(r_{cr})$, which is small compared with both r_a/\dot{r}_a and W/\dot{W} ; r_{cr} is the radius at the critical density ρ_{cr} , $r_a(t)$ is the target or ablation radius, and $W(t)$ is the absorbed power. Using momentum conservation the first condition reads $r_{cr}/r_a \ll v(r_{cr})/\dot{r}_a \sim |\rho(r_a)/\rho_{cr}|^{1/2}$ and is usually satisfied: compression may increase $\rho(r_a)$ well above solid density, which, for $1.06 \mu\text{m}$ light and an Al target, say, is about $770 \rho_{cr}$. Note that if the pulse lasts throughout the entire collapse we have $W/\dot{W} \sim r_a/\dot{r}_a$.

For $\rho(r_a)/\rho_{cr} \rightarrow \infty$ the fluid model is quite simple. Because of the nonlinear character of heat conductivity,⁵ $K = \bar{K}T^{5/2}$, a sharp ablation front at r_a uncouples the pellet from the corona. The corona is then parametrized by a dimensionless number,^{2,4} $\hat{W}(W, r_a, n_{cr}, Z_i, \bar{m}) \equiv W/r_a^2 \rho_{cr} V^3$, where ρ_{cr} is $\bar{m}n_{cr}$, Z_i is the ion charge number, $\bar{m} \equiv m_i/Z_i$ is the mass per unit charge, and V is a convenient speed,⁶

$$\begin{aligned} V &\equiv \left(\frac{r_a n_{cr}}{\bar{m}^{5/2} \bar{K}(Z_i)} \right)^{1/4} \\ &= \frac{\pi^{7/8} c}{5^{1/4} 2^{7/8}} \left(\frac{m_e}{\bar{m}} \right)^{5/8} \left(\frac{r_a}{n_{cr} \lambda^4} \frac{Z_i \ln A}{\epsilon \delta_T} \right)^{1/4} \\ &\approx 0.936 \times 10^7 \frac{\text{cm}}{\text{sec}} \left(\frac{2Z_i}{A_i} \right)^{5/8} \left(\frac{1.06 \mu\text{m}}{\lambda} \right)^{1/2} \\ &\quad \times \left(\frac{r_a}{100 \mu\text{m}} \frac{Z_i \ln A}{100 \epsilon \delta_T} \right)^{1/4}; \end{aligned} \quad (1)$$

$\ln A$, ϵ , δ_T ,⁵ m_e , and c have the usual meaning.

The continuum model fails above some \hat{W} because the ratio of mean free path to hydrodynamic scale ceases to be small somewhere in the corona, making the classical formula for the heat flux, $q = -\bar{K}T^{5/2} \times dT/dr$, inaccurate. A crude recipe for this failure,^{3,4} in order to saturate the flux ($|q| < f n T^{3/2} m_e^{-1/2}$),⁷ calls for a difficult choice of the factor f . For slab experiments, simulation⁷ and analytical⁸ results have suggested $f \approx 0.03$ but controversy on this point persists.⁹ In addition, the value of f to use might change with the geometry; taking it independent of position is an overall sim-

plification. (This guess is confirmed in pellet experiments by Goldsack *et al.*¹⁰; $f = 0.03$ simulations disagreed with the data, but agreement was attained with $f = 0.1$.)

Actually most overall results for pellets are only "piecewise" sensitive to the value of the saturation factor.⁴ In particular, the relation between mass ablation rate \dot{m} and ablation pressure P_a is independent of f for $f > 0.05$ roughly; $P_a(W)$ is nearly independent of f for $f > 0.08$ and $\hat{W} < 10^4$. The relation between the critical radius r_{cr} and W is only weakly dependent on f .^{11,12} These results are in accordance with the findings in Ref. 10, where agreement between data and simulations was attained for all $f > 0.1$. In these experiments, $5 < \hat{W} < 5 \times 10^3$.

Thus if f is not too low, the classical heat flux (formally corresponding to the limit $f \rightarrow \infty$) may be used to calculate overall relations. The exception¹³ is $P_a(W)$ at $\hat{W} > 10^4$. To understand why this relation is sensitive to the value of f , note that if saturation is ignored (a) the enthalpy and kinetic-energy fluxes are continuous at r_{cr} , while dT/dr is not, so that $W/4\pi r_{cr}^2 = q(r_{cr}^+) - q(r_{cr}^-)$; and (b) if \hat{W} is well above 10^4 (or r_{cr}/r_a above 3) roughly, we have $q(r_{cr}^+) \approx W/4\pi r_{cr}^2 > |q(r_{cr}^-)|$.² Saturation then mainly affects the huge outward heat loss, increasing $4\pi r_{cr}^2 |q(r_{cr}^-)|/W$ and thus P_a , to an extent sensitive to the value of f : for $\hat{W} \sim 10^7$, P_a shows a three-fold increase as f grows from 0.06 to 0.35.⁴ In this paper we explore this high \hat{W} regime with a model that makes no appeal to flux saturation. The model is based on the appearance of suprathermal electrons; crucial to the determination of $P_a(W)$ is the magnitude of the outward (not the inward) energy transport by these electrons. At the end we compare our results with results from a one-temperature, saturated-flux model.

II. PHYSICAL MODEL

A basic analysis ought to include a kinetic evaluation of q under weakly collisional conditions. We look, however, for a simple description, and bypass this current, important problem. The fluid model is modified to allow for two convenient facts:

(i) For $f \gtrsim 0.1$, saturation starts in the underdense region, at $\hat{W} \approx 10^3$ (Fig. 9, Ref. 4); overdense saturation starts at much higher values ($\sim 10^7$ for $f \approx 0.3$). For the intermediate regime, evaluation of q is a problem only for $r > r_{cr}$; for

$r < r_{cr}$, collisions are frequent enough to warrant a continuum description. This fact is tied to the result $q(r_{cr}^+) \gg |q(r_{cr}^-)|$ (Sec. I).

(ii) For high intensities, resonant absorption generates suprathermal or hot electrons of temperature $T_H \gg T_C \equiv T(r_{cr})$, T being now the main (cold) temperature.¹⁴⁻¹⁶ For $r > r_{cr}$, hot electron collisions may be neglected. A large ambipolar field will build up to preserve quasineutrality.

The main consequence of these facts is that the overdense coronal flow is controlled by collision-dominated cold electrons and the underdense flow by collisionless hot electrons.

A. Overdense corona

Hot electrons entering this region are assumed to contribute negligibly to macroscopic quantities. This assumption is checked at the end. Cold electrons are treated as a continuum fluid with heat flux $-\bar{K}T^{5/2} dT/dr$. The equations for the ion-electron fluid are^{1,2}

$$r^2 Z_i n_i v = \mu \equiv m/4\pi\bar{m} \quad (Z_i n_i \simeq n), \quad (2)$$

$$\bar{m} n v \frac{dv}{dr} = -\frac{d(nT)}{dr}, \quad (3)$$

$$n v \left(\frac{1}{2} \bar{m} v^2 + \frac{5}{2} T \right) - \bar{K} T^{5/2} \frac{dT}{dr} = 0. \quad (4)$$

Both T and q vanish at the cold ablation radius r_a . We neglect electron inertia, assume spherical symmetry, and take Z_i large in order to uncouple the ion temperature (the only quantity sensitive to the charge number).⁴

Let r_a , n_{cr} , Z_i , \bar{m} , and P_a , though not W , be given. Choosing a value for \bar{m} or μ , Eqs. (2)–(4) can be integrated from r_a outward to obtain flow profiles; \bar{m} is then determined by requiring the solution to be univalued at the sonic point. Equation $n(r_{cr}) = n_{cr}$ yields r_{cr} and both T_C and $v_{cr} \equiv v(r_{cr})$.

Evaluating (4) at r_{cr}^- and using $\bar{K}T^{5/2} \simeq 17.02\epsilon\delta_T l_{ei} n (T/m_e)^{1/2}$,³ where l_{ei} is the ion-electron mean free path, yields

$$\frac{l_{ei}}{r_{cr}} = \frac{5}{2} \left(\frac{m_e}{\bar{m}} \right)^{1/2} M_C \left(1 + \frac{M_C^2}{5} \right) \frac{d \ln r / d \ln T}{17.02\epsilon\delta_T}, \quad (5)$$

where $M_C^2 \equiv \bar{m} v_{cr}^2 / T_C$; for an Al target,

$$\frac{l_{ei}}{r_{cr}} \simeq 7.9 \times 10^{-3} M_C (1 + M_C^2/5) \frac{d \ln r}{d \ln T}.$$

Later we will consider $4 < \eta_{cr} < 9$; then $0.19 > d \ln T / d \ln r > 0.08$, $5 < M_C^2 < 8$ (see Fig. 2 of Ref. 2), and $0.19 < l_{ei}/r_{cr} < 0.72$. Thus the plasma is barely collisional at r_{cr} (of course, l_{ei}/r decreases rapidly with decreasing r); the fact, however, that $d \ln T / d \ln r \ll 1$ at r_{cr}^- makes the heat-flux classical for $r < r_{cr}$, if f is not too low.

B. Underdense corona

Next, consider $r > r_{cr}$. The energy equation now reads

$$4\pi r^2 (n v \frac{1}{2} \bar{m} v^2 + n \frac{5}{2} T + q) = W. \quad (6)$$

For low powers, $q = -\bar{K}T^{5/2} dT/dr$, and Eqs. (2), (3), and (6), with boundary condition $T(r \rightarrow \infty) \rightarrow 0$, would yield W^2 . For \bar{W} above 10^4 , however, saturation sets in at r_{cr}^+ for all f ;

evaluating (6) at r_{cr}^+ with $q = f n T^{3/2} / m_e^{1/2}$ yields W^4

$$\bar{m} \left[\frac{1}{2} v_{cr}^2 + \frac{T_C}{2\bar{m}} \left(5 + f \frac{2T_C^{1/2}}{m_e^{1/2} v_{cr}} \right) \right] = W. \quad (7a)$$

Unfortunately, when values $0.03 < f < 0.6$ are allowed for, the indeterminacy in the relation $W(P_a)$ is too large, as shown in Sec. I [the factor $(4T_C/m_e v_{cr}^2)^{1/2}$ is large].

In this paper we use the energy equation at r_{cr}^+ in the form

$$\bar{m} [\frac{1}{2} v_{cr}^2 + (T_H/2\bar{m})(5 + \beta)] = W, \quad (7b)$$

where β is a factor of order unity. This amounts to writing the heat flux as

$$q = n v (\beta/2) T \quad (8)$$

and choosing T_H from between the two temperatures of our model for both enthalpy and heat fluxes. Equation (7b) closes the problem if T_H is known.

Equation (8) has been used both in astrophysical and laser-fusion applications. The electron distribution function $F(u, r, t)$ is given by

$$\left(\mathbf{u} \cdot \nabla + \frac{e}{m_e} \nabla \psi \cdot \frac{\partial}{\partial \mathbf{u}} \right) F = \frac{\delta F}{\delta t} \quad (9)$$

which is a steady Vlasov equation if time variations and collisions, represented by $\delta F/\delta t$, are neglected. Unsteady effects are weak because r_a and W change slowly (Sec. I). Collisional effects are stronger for cold electrons. They will be small if $|e \nabla \psi| F / (m_e T_C)^{1/2} \gg (T_C/m_e)^{1/2} F / l_{ei}$; this condition becomes $T_H/T_C \gg r_{cr}/l_{ei} \sim 2$. In order to preserve quasineutrality in the presence of hot electrons we must have $|e \nabla \psi| \sim T_H/r_{cr}$.

The steady Vlasov equation clearly yields zero odd moments for F (current, enthalpy flux, heat flux).^{17,18} Corrections caused by $\delta F/\delta t$ will then give small odd moments of same order.¹⁷ Now, the electron flux at r_{cr}^+ is known from the conditions of zero total current: $\int F u_r du = n_{cr} v_{cr}$, where u_r is the radial component of \mathbf{u} . Further, since $|e \nabla \psi| \gg T_C/r_{cr}$, odd moments of F , caused by electrons leaking out to infinity, will arise from the hot population. Then, we have at r_{cr}^+ the enthalpy flux $\simeq n_{cr} v_{cr} \frac{5}{2} T_H$ and the heat flux $\simeq n_{cr} v_{cr} (\beta/2) T_H$,¹⁷ leading to (7b).

C. Hot electron temperature

We take T_H from simulations^{14,15} that give

$$T_H \simeq A T_C^\gamma (1 \text{ keV})^{1-\gamma} (I_{cr} \lambda^2 / 10^{15} \text{ W cm}^{-2} \mu\text{m}^2)^\alpha, \quad (10)$$

where $\gamma = \frac{1}{2}$, $\alpha = \frac{1}{3}$, $A = 6.5$,¹⁴ or $\gamma = 0.25$, $\alpha = 0.39$, $A = 8.7$ (Ref. 15). Here $I_{cr} = W/4\pi r_{cr}^2 \phi$ and ϕ is the absorption fraction. Equation (10) must be fitted into a basic form. If E and L are the field and length of the resonant plasma wave, then $T_H \sim eEL$. Here, L/λ is a function of $m_e c^2/T_C$ and $I_{cr}/cn_{cr} T_C$ (Ref. 14); we also have $E^2 \propto I_{cr}/c$ (Ref. 14), or $E^2 \propto I_{cr}/(T_H/m_e)^{1/2}$.¹⁶ For a restricted parameter range we may then write

$$T_H \simeq B T_C^\gamma (I_{cr}/cn_{cr})^\alpha (m_e c^2)^{1-\gamma-\alpha}. \quad (11a)$$

Comparing (10) and (11a) we obtain $T_H \propto c^{1/3}$ for both $\gamma = \frac{1}{2}$ and $\gamma = 0.25$. Accordingly we set $\alpha = (5 - 6\gamma)/9$.

We rewrite (11a) in the form

$$T_H \simeq B \left(\frac{m_e}{\bar{m}} \right)^{(1-3\gamma)/9} \frac{T_c^\gamma (\bar{m} V^2)^{1-\gamma}}{(\bar{m} V / m_e c)^{1/3}} \left(\frac{\hat{W}}{4\pi\phi} \frac{r_a^2}{r_{cr}^2} \right)^{(5-6\gamma)/9} \quad (11b)$$

Equation (11b) shows that resonant absorption effects are parametrized by the dimensionless number $\hat{V} \equiv \bar{m} V / m_e c$. (Inverse bremsstrahlung effects are parametrized by \bar{V} , too.¹²) We use (11b) in (7b). To make (11b) agree with (10), to within 1% for both $\gamma = \frac{1}{3}$ and $\gamma = 0.25$, we set $B(\bar{m}/m_e)^{(1-3\gamma)/9} = 1.35$.

III. OVERDENSE HOT EFFECTS

We now justify neglecting hot electron effects in the overdense region. For simplicity, we estimate them assuming that ingoing hot electrons at r_{cr} are isotropic and mono-energetic. They scatter off high- Z_i ions at a rate determined by the 90°-deflection time $t_D = m_e^2 \omega^3 / 8\pi Z_i n e^4 \ln \Lambda$,⁵ and lose energy to cold electrons at a slower rate of characteristic time $Z_i t_D$; $E_H \equiv \frac{1}{2} m_e \omega^2$ is the hot energy. Then

$$\frac{d\langle s^2 \rangle}{dt} = \omega^2 t_D = \frac{2E_H t_D}{m_e}, \quad (12)$$

$$\frac{dE_H}{dt} = \frac{-E_H}{Z_i t_D}, \quad (13)$$

where $\langle s^2 \rangle$, the mean squared distance from r_{cr} , obeys a random-walk law. We assume that hot electrons remain "marked hot" as they lose energy (see Ref. 3 for an alternative description). Then we have

$$\text{hot density} \equiv n_H(r) \simeq n_H(r_{cr}). \quad (14)$$

For electrons moving radially on the average we set $\langle s^2 \rangle = (r_{cr} - r)^2$. From (12) and (13), we obtain

$$\frac{dE_H}{dr} = \frac{m_e (r_{cr} - r)}{Z_i t_D^2}. \quad (15)$$

The largest hot electron effects on the ion-plus-cold-electron fluid should be caused by energy exchange. Hence, we neglect hot density, current, and pressure, against the corresponding cold quantities. We neglect $3T/2$ against E_H also. Consequently (4) becomes

$$\frac{1}{r^2} \frac{d}{dr} r^2 \left[n v \left(\frac{1}{2} \bar{m} v^2 + \frac{5}{2} T \right) - \bar{K} T^{5/2} \frac{dT}{dr} \right] = \frac{n_H E_H}{Z_i t_D}; \quad (16)$$

Eqs. (2) and (3) are not modified. The analysis of the overdense region is then given by Eqs. (2)–(4) for $r_a^* < r < r_{th}$, and by (2), (3), (16), (14), and (15) for $r_{th} < r < r_{cr}$. The boundary condition on (15) is $E_H(r_{cr}) = 3T_H/2$; r_{th} is determined by a thermalization condition, $E_H(r_{th}) = 3T(r_{th})/2$.

We carried out calculations for different values of $n_H(r_{cr})/n_{cr}$. For low values we obtain the cold n, v, T profiles, as well as r_{th} , and E_H for $r_{th} < r < r_{cr}$. As $n_H(r_{cr})/n_{cr}$ increases the profiles change and the power going into the cold electrons ($4\pi r_{cr}^2 \times \bar{K} T_c^{5/2} dT/dr|_{r_{cr}}$) decreases. This power vanishes at about $n_H(r_{cr})/n_{cr} = \frac{1}{3}$. At this point, the overall relations $r_{cr}(W)$ and $P_a(W)$ differ by a few percent from results that ignore hot-energy deposition, even though the ion-

plus-cold-electron flow is sensibly modified. We conclude that overdense hot effects *may* be neglected for all reasonable values of $n_H(r_{cr})/n_{cr}$, which is a free parameter of the analysis. We found $r_{th} > r_a$ always.

IV. DISCUSSION

Figure 1(a) and (b) shows r_{cr}/r_a and $P_a/\rho_{cr} V^2$ vs \hat{W} for a few values of \hat{V} . Numerically

$$\hat{W} \simeq \frac{0.682 W}{10^9 \text{ watts}} \left(\frac{A_i}{2Z_i} \right)^{7/8} \left(\frac{\lambda}{1.06 \mu\text{m}} \right)^{7/2} \times \left(\frac{100 \mu\text{m}}{r_a} \right)^{11/4} \left(\frac{100 \epsilon \delta_T}{Z_i \ln \Lambda} \right)^{3/4}, \quad (17)$$

$$\hat{V} \simeq 1.14 \left(\frac{A_i}{2Z_i} \right)^{3/8} \left(\frac{1.06 \mu\text{m}}{\lambda} \right)^{1/2} \left(\frac{r_a}{100 \mu\text{m}} \frac{Z_i \ln \Lambda}{100 \epsilon \delta_T} \right)^{1/4}. \quad (18)$$

Results from Ref. 4 for several values of f are also shown for comparison.¹⁹

Both the present and the saturated-flux, one-temperature, models are simple approximations. For the second one,

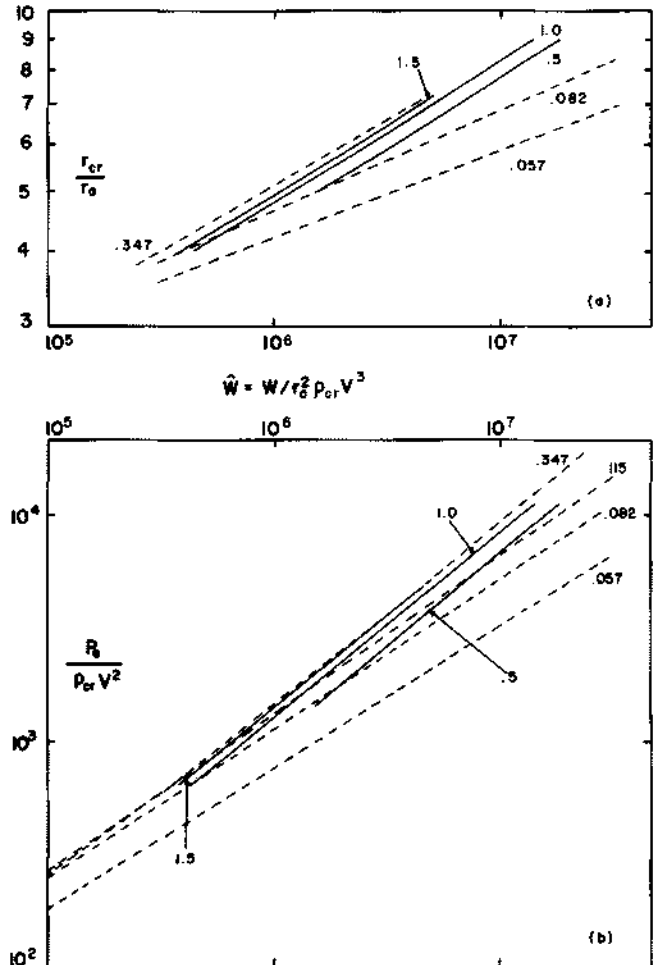


FIG. 1. Critical radius r_{cr} (a) and ablation pressure P_a (b) versus absorbed laser power W , as found here (—) and in Ref. 4 (---) for a few values of \hat{V} and $f(A_i/2Z_i)^{1/2}$, respectively. Here, V , \hat{W} , and \hat{V} are defined in Eqs. (1), (17), and (18); f is the flux saturation factor, r_a is the ablation radius, ρ_{cr} is the mass critical density, and A_i and Z_i are the ion mass and charge number, respectively.

however, we still have to choose a value for f ; this is certainly a questionable matter for pellets and makes results at high \hat{W} useless. Figure 1(b) shows that for $\hat{W} = 10^7$, P_a increases by a factor of 3 in going from $f \approx 0.06$ to $f \approx 0.35$ [r_{cr} in Fig. 1(a) increases by a factor of 1.5]; when values $f = 0.03$ and 0.6 are considered^{3,4} the factor is larger than 10 (a 1000% indeterminacy). In the present model \hat{V} is a known parameter. The indeterminacy arises from 10% errors in the approximations, and from the factor $(1 + \beta/5)\phi^{(6\gamma-5)/9}$, after using (11b) in (7b). To draw Fig. 1 we set $\beta = 0$, $\phi = 0.4$, and checked that P_a and r_{cr} changed by 15% and 5%, respectively, for $\beta = \pm 1$; for $\phi = 0.5$ or 0.3 , changes were half as large. There is no reason to expect β to be large. Thus, results should be accurate to within 50% at worst. From Fig. 1 we may conclude that the saturated-flux model with $f = 0.03$ or 0.6 does not agree with the present model; agreement requires setting $f = 0.1$ to 0.3 .

Our analysis requires a profile steepening at r_{cr} that is neither too weak (resonant absorption and electron acceleration must be significant) nor too strong (the upper density in the step profile must be close to n_{cr} , as is implicitly assumed in the model). This was ensured by making $I_{cr}\lambda^2$ lie between the lowest values studied in Refs. 15 and 14 (0.3 and 5×10^{15} W cm⁻² μ m², respectively); in all cases $I_{cr}/cn_{cr}T_C$ lay between its lowest values in Ref. 15 (0.05) and Ref. 14 (0.4) [accordingly we set $\gamma = 0.25$ in (11b)]. The range of validity of present results starts at about $\hat{W} \approx 3 \times 10^5$ and reaches above 10^7 ; it extends significantly the results from Refs. 2, 4, and 12, which extended up to about 3×10^4 .

The range depends on \hat{V} as is roughly shown in Fig. 1; it narrows at both low and high \hat{V} . This is because $\hat{W} \propto I_{cr}\lambda^2 \hat{V}^{-3}$. At low \hat{V} , and for $I_{cr}\lambda^2$ at its upper bound, \hat{W} (or r_{cr}/r_a) is too large; I_{cr}/r_{cr} exceeds unity and Spitzer's flux fails at r_{cr}^- . At high \hat{V} and $I_{cr}\lambda^2$ at its lowest

bound, r_{cr}/r_a is too low: hot electrons thermalize at r_{cr} ($r_{th} \approx r_{cr}$). Fortunately \hat{V} is close to unity for most experiments of interest.

ACKNOWLEDGMENT

This research was sponsored by the Comisión Asesora de Investigación Científico-Técnica of Spain.

¹Yu. V. Afanas'ev, E. G. Gamalii, O. N. Krokhin, and V. B. Rozanov, Sov. Phys. JETP **44**, 311 (1977); S. J. Gitomer, R. L. Morse, and B. S. Newberger, Phys. Fluids **20**, 234 (1977).

²J. Sanz, A. Liñán, M. Rodríguez, and J. R. Sanmartín, Phys. Fluids **24**, 2098 (1981).

³C. E. Max, C. F. McKee, and W. C. Mead, Phys. Fluids **23**, 1620 (1980).

⁴J. Sanz and J. R. Sanmartín, Phys. Fluids **26**, 3361 (1983).

⁵L. Spitzer, *Physics of Fully Ionized Gases* (Wiley, New York, 1967), Chap. 5.

⁶In Eq. (20) of Ref. 4, defining V , the exponent $\frac{1}{2}$ was missing from \bar{m} . Here temperature T is measured in energy units.

⁷W. L. Kruer, Comments Plasma Phys. **5**, 69 (1979).

⁸R. Ramis and J. R. Sanmartín, Nucl. Fusion **23**, 739 (1983).

⁹N. St. J. Braithwaite, A. Montes, and L. M. Wickens, Plasma Phys. **23**, 713 (1981).

¹⁰T. J. Goldsack, J. D. Kilkenny, B. J. MacGowan, P. F. Cunningham, C. S. Lewis, M. H. Key, and P. T. Rumsby, Phys. Fluids **25**, 1634 (1982).

¹¹See Figs. 10 and 11 of Ref. 4.

¹²In Refs. 1-4 absorption was assumed to occur at n_{cr} . Inverse bremsstrahlung absorption at $n < n_{cr}$ has been studied by J. Nicolás and J. R. Sanmartín, submitted to Plasma Phys. and Controlled Fusion.

¹³Since $m(P_a)$ is independent of f , $m(W)$ will depend on f , too.

¹⁴D. W. Forslund, J. M. Kindel, and K. Lee, Phys. Rev. Lett. **39**, 284 (1977).

¹⁵K. Estabrook and W. L. Kruer, Phys. Rev. Lett. **40**, 42 (1978).

¹⁶J. R. Albritton and A. B. Langdon, Phys. Rev. Lett. **45**, 1794 (1980).

¹⁷E. J. Valeo and I. B. Bernstein, Phys. Fluids **19**, 1348 (1976).

¹⁸P. Mora and R. Pellat, Phys. Fluids **22**, 2300 (1979).

¹⁹The relations between r_{cr}/r_a and $P_a/\rho_a V^2$, and r_{cr}/r_a and $m/r_a^2 \rho_{cr} V$ are the same as in Ref. 2, because the overdense analysis is the same.

